Hindawi
Journal of Nanomaterials
Volume 2017, Article ID 7209489, 7 pages
https://doi.org/10.1155/2017/7209489

Research Article

Probing the Effect of Ag_2S Quantum Dots on Human Serum Albumin Using Spectral Techniques

Yiying Fu, Enli Guan, Jiangong Liang, Guolan Ren, and Lu Chen

College of Science, Huazhong Agricultural University, Wuhan 430070, China

Correspondence should be addressed to Guolan Ren; renguolan@mail.hzau.edu.cn and Lu Chen; chenlu@mail.hzau.edu.cn

Received 4 January 2017; Accepted 8 February 2017; Published 6 March 2017

Academic Editor: Run Zhang

The understanding of the interaction between protein and quantum dots (QDs) has significant implications for biological applications of QDs. Herein, we studied the effect of Ag_2S QDs on human serum albumin (HSA) using UV-Vis absorption spectra and fluorescence spectroscopy and found that the fluorescence intensity of HSA was gradually decreased with increasing Ag_2S QDs concentrations. By using the Stern-Volmer equation for the fluorescence quenching constant (K_{SV}) of the response of Ag_2S QDs to HSA as well as thermodynamic equations, the values of thermodynamic enthalpy change (ΔH^{θ}), entropy change (ΔS^{θ}), and free energy change (ΔG^{θ}) were calculated to be $-10.79\ \mathrm{KJ{\cdot}mol^{-1}}$, $37.80\ \mathrm{J{\cdot}mol^{-1}{\cdot}K^{-1}}$, and $-22.27\ \mathrm{KJ{\cdot}mol^{-1}}$, respectively. The results indicate that Ag_2S QDs exert an obvious static fluorescence quenching effect on HSA and electrostatic interaction plays a key role in the binding process. Furthermore, Raman spectral analysis reveals that Ag_2S QDs alter the external environment of tyrosine and tryptophan or the C-H bending of HSA but not the α-helical content.

1. Introduction

With the wide application of QDs in the biological system, their biological effects have attracted increasing attention [1]. Up to now, several papers have reported the effects of QDs on proteins, DNA, cells, and so forth. [2–7], and obvious biological toxicity of QDs has been detected and confirmed. For example, Shen et al. have studied the interaction between human hemoglobin and CdS QDs by spectroscopic analysis and confirmed that both electrostatic forces and chemical bonds play an important role in the interaction [6]. Luo's group investigated nonspecific interactions between QDs and proteins by atomic force microscopy and found that van der Waals forces were the leading forces for the interaction, while electrostatic interactions also played a key role [8]. Wang et al. investigated the effects of CdSe/ZnS QDs on human blood serum and found that a hard protein corona was formed by irreversible binding [9]. In our recent study, the interaction between CdTe QDs and protamine sulfate has been examined, and a combined dynamic and static quenching model was proposed [10]. Li et al. found that TGA-capped CdTe QDs could induce DNA damage and apoptosis of hepatocyte line HL-7702 [11]. Xu et al. investigated the toxicity of CdTe QDs capped with three different reagents on engineering *Escherichia coli* based on protein expression and found that CdTe QDs capped with mercaptoacetic acid have more toxicity than those capped with glutathione and L-cysteine [12]. Despite many studies on the interaction between QDs and the biological system, more detailed investigations are still necessary due to effects of many factors such as the size, surface charge, and structure of QDs on their toxicity [13, 14].

Ag_2S QDs are good alternatives for fluorescence detection and imaging of biological molecules due to their excellent properties such as small size, near-infrared emission, and low toxicity [15–17]. Many previous studies focused on the synthesis and application of Ag_2S QDs [18–20]. For example, Li et al. have successfully synthesized near-infrared Ag_2S QDs with high tumor target ability by injecting Ag_2S QDs fluorescence probe to mice with tumor and obtained good results in in vivo imaging and dynamic tracking [17]. Ag_2S QDs based fluorescence probes have shown great potential applications not only in in vivo imaging, but also in biomedical research and disease diagnosis [21]. These studies have

shown potential biological applications of Ag_2S QDs, but their potential toxicity and effectiveness in biological systems remain to be elucidated, implying the necessity to understand the interaction of Ag_2S QDs with protein and its mechanism in biomedical applications.

Human serum albumin (HSA) consists of 585 amino acids [22], with a molecular weight of about 66 kD [23], and 17 disulfide bonds which can be folded to form three regions. There are nine annular regions in HSA, with three rings in each region [24–26]. HSA has an alpha helical structure which can be flexibly reversed to subdomains [27]. Due to the presence of tryptophan, tyrosine, and phenylalanine, HSA can emit strong fluorescence under 280 nm excitation [24]. Usually, the contribution ratio of fluorescence intensity of phenylalanine, tyrosine, and tryptophan is 0.5 : 9 : 100, indicating that the fluorescence of HSA is mainly derived from its tryptophan residues. Furthermore, the tryptophan residues are sensitive to surrounding environments, which directly leads to changes in the fluorescence intensity of HSA [28].

In the present work, the interaction between Ag_2S QDs and HSA was investigated using UV-Vis absorption spectra, fluorescence spectroscopy, and Raman spectra. The Ag_2S QDs were found to have obvious fluorescence quenching effects on HSA at different temperatures (e.g., 297 K, 305 K, and 313 K). The fluorescence quenching mechanism and the thermodynamic mechanism were also systematically investigated.

2. Materials and Methods

2.1. Materials and Equipment. Silver nitrate, nitric acid, isopropyl alcohol, glutathione (GSH), and $NaH_2PO_4{\cdot}2H_2O$ were obtained from Sinopharm Chemical Reagent Co., Ltd. (Shanghai, China). $Na_2HPO_4{\cdot}12H_2O$ was purchased from Shanghai Xinhua chemical plant (Shanghai, China). Sulfur powder was acquired from Tianjin Sea Crystal Fine Chemical Co., Ltd. (Tianjin, China); $N_2H_4{\cdot}H_2O$ was purchased from Tianjin Bodi Chemical Co., Ltd. (Tianjin, China); and human serum albumin (HSA) was obtained from Shanghai Bo'ao Biological Technology Co., Ltd. (Shanghai, China). Ultrapure water (Milli-Q, Millipore, 18.2 MΩ resistivity) was used as the experimental water.

The equipment used included an FLSP920 spectrometer (Edinburgh Instruments), Malvern Zetasizer instrument (Malvern ZEN 3690), FEI Talos F200C transmission electron microscope (FEI Co.), MicroUV-2450 UV visible spectrophotometer (Unocal Shanghai Instrument Co. Ltd.), inductively coupled plasma atomic emission spectrometer (IRIS Intrepid II XSP, Thermo Fisher Scientific, USA), Raman spectrometer (Renishaw, UK) equipped with a confocal microscope (Leica, Germany), DF-101S collector type constant temperature heating magnetic agitator, AL204 electronic balance (Mettler Toledo Instruments Shanghai Co. Ltd.), and GL-21M intelligent high speed refrigerated centrifuge (Changsha Ordinary Instrument Limited Company).

2.2. Experimental Section

2.2.1. Preparation and Characterization of Ag_2S QDs. Ag_2S QDs were synthesized as previously reported with some modifications [29]. Briefly, 0.160 g S powder was mixed with 10 mL hydrazine hydrate in a beaker, followed by stirring the mixture overnight at room temperature. Next, 0.192 g of GSH and 0.043 g of $AgNO_3$ were dissolved in 25 mL ultrapure water at three flask reactors until the solid was completely dissolved. Under N_2 protection, the solution was supplemented with 0.050 mL of the aqueous S^{2-} source. After 30 min, the Ag_2S QDs were obtained at the centrifugal separation speed of 8000 r/min after washing in isopropyl alcohol. The precipitation was redissolved in 30 mL aqueous phase to obtain Ag_2S QDs solution, which was kept in a refrigerator at 277 K until use. The size and concentration of Ag_2S QDs were determined by transmission electron microscopy (TEM) and inductively coupled plasma atomic emission spectrometer (ICP-AES).

2.2.2. Investigation of the Interaction between Ag_2S QDs and HSA. HSA and different concentrations of Ag_2S QDs were mixed in a 5.0 mL colorimetric tube in buffer solutions and reacted for 30 min. After that, the HSA fluorescence intensity was recorded at 280 nm. The effects of temperature on the reaction system were investigated by repeating the above steps separately at 297, 305, and 313 K.

The Raman spectra were recorded with inVia micro-Raman spectroscopy. The mixture was composed of HSA and Ag_2S QDs at concentrations of 1.0×10^{-5} mol/L and 1.0×10^{-4} mol/L, respectively. Next, the mixture was dropped onto the foil. After the liquid was dried, the Raman spectra were recorded at the excitation wavelength of 633 nm.

3. Results and Discussion

3.1. Characterization of Ag_2S QDs. The size of Ag_2S QDs was determined by transmission electron microscopy. From Figure 1(a), it can be seen that the average size of Ag_2S QDs was 3.4 ± 0.2 nm. The top right corner of Figure 1(a) presents the hydrodynamic size distribution images of Ag_2S QDs, which reveals that the diameter of the QDs is in the range of 3–7 nm with an average size of 4.7 nm. The as-prepared Ag_2S QDs are consistent with those described in the literature [29].

As shown in Figure 1(b), the UV-Vis absorption spectrum of Ag_2S QDs was in the absorption range of 250 nm and 300 nm, and there was a small peak centered at 270 nm. The normalized fluorescence emission spectrum of resultant Ag_2S QDs in aqueous solution was also displayed in Figure 1(b). When these Ag_2S QDs were excited under UV irradiation with 450 nm excitation wavelength, the maximum emission peak at 700 nm was observed.

3.2. The Quenching Effects of Ag_2S QDs on the Fluorescence of HSA. As shown in Figure 2, with the steady increase of Ag_2S QDs concentration and the decrease of HSA fluorescence intensity, Ag_2S QDs showed strong quenching effects on the fluorescence of HSA. HSA molecules can emit strong intrinsic fluorescence due to the presence of tryptophan

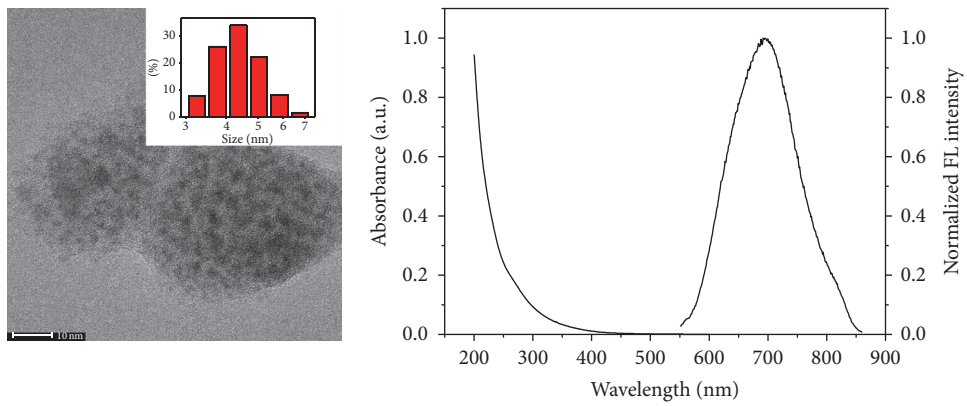

Figure 1: (a) The TEM image of Ag_2S QDs (the inset shows the hydrodynamic size distribution of Ag_2S QDs). (b) The UV-Vis absorption spectrum and the fluorescence emission spectrum of Ag_2S QDs.

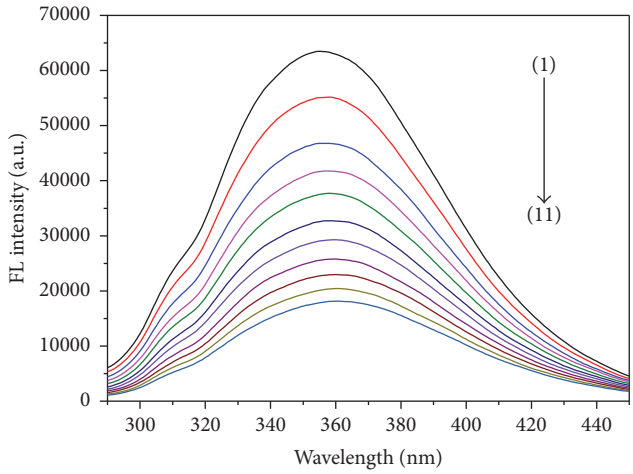

Figure 2: Fluorescence spectra of HSA at different concentrations of Ag_2S QDs. (λex = 280 nm, λem = 360 nm, $C_{(HSA)} = 4.2 \times 10^{-7}$ mol/L, $C_{(Ag_2S)}$(1–11): 0, 3.0, 6.0, 9.0, 12.0, 15.0, 18.0, 21.0, 24.0, 27.0, and 30.0 $\times 10^{-5}$ mol/L, pH = 7.4, T = 297 K).

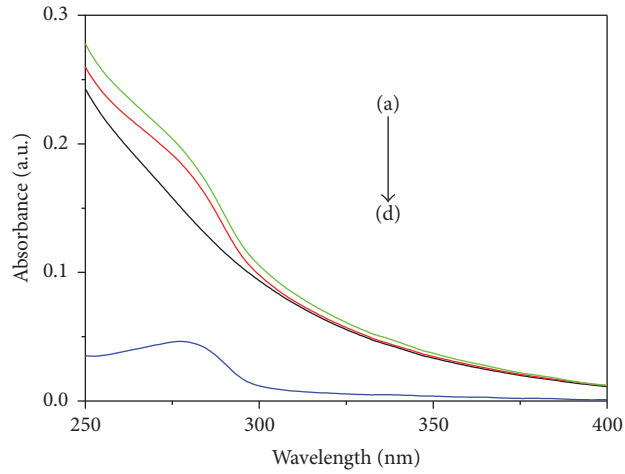

Figure 3: (a) The overlaying UV-Vis absorption spectrum of Ag_2S QDs and HSA. (b) The UV-Vis absorption spectrum after reaction. (c) The UV-Vis absorption spectrum of Ag_2S QDs. (d) The UV-Vis absorption spectrum of HSA ($C_{(HSA)} = 8.4 \times 10^{-7}$ mol/L, $C_{(Ag_2S)} = 3.0 \times 10^{-4}$ mol/L, pH = 7.4).

residues. When combined with Ag_2S QDs, the interaction led to alterations in the external environment and structure of the protein, resulting in the decrease of fluorescence intensity. With the increase of Ag_2S QDs concentration, the HSA peak shape and the maximum emission peak remained unchanged.

3.2.1. Investigation of the Quenching Mechanism. The dynamic quenching only affects the fluorescent molecules and does not change the UV-Vis absorption spectra of fluorescent materials. The UV-Vis absorption spectra of fluorescent materials are changed due to static quenching, which results from the formation of complexes [7, 21]. Based on this theory, if the UV-Vis absorption spectra of HSA and the complexes of QDs and HSA vary with each other, the quenching mechanism should be static quenching [30].

The UV-Vis absorption spectrum after reaction was recorded between 250 and 400 nm (Figure 3(b)). The sum of the absorption spectrum intensity of HSA (Figure 3(d)) and the absorption spectrum intensity of Ag_2S QDs (Figure 3(c)) is shown in Figure 3(a). With the addition of Ag_2S QDs, the absorption spectrum of the mixture was different from that of the sum of the individual spectra of both Ag_2S QDs and HSA, which can be attributed to the interaction between QDs and protein, demonstrating that HSA fluorescence quenching by Ag_2S QDs is a static procedure.

3.2.2. The Effect of Temperature. Basically, fluorescence quenching can be divided into static and dynamic quenching. In static quenching, the quencher reacts with the ground-state fluorescent molecule and forms a complex, while in dynamic

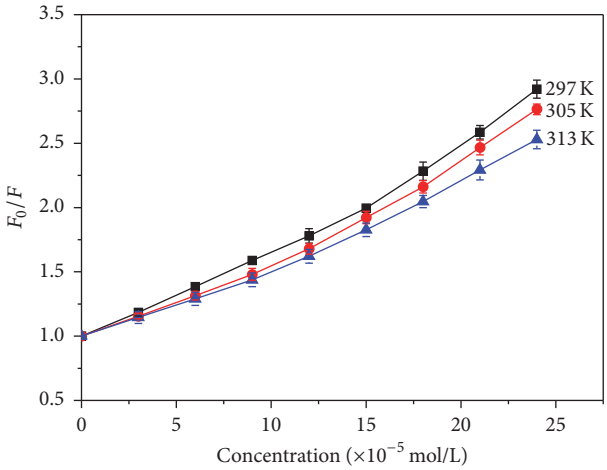

Figure 4: Stern-Volmer equation at different temperatures (λex = 280 nm, λem = 350 nm, $C_{(HSA)} = 4.2 \times 10^{-7}$ mol/L, pH = 7.4).

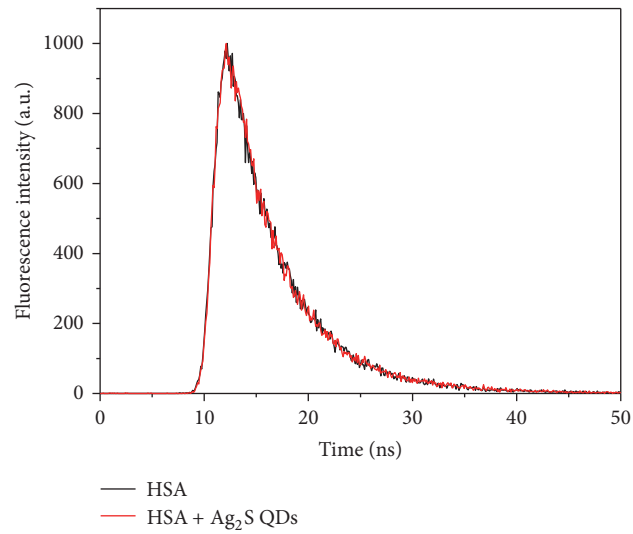

Figure 5: The fluorescence lifetime of HSA in the absence and presence of Ag_2S QDs ($C_{(HSA)} = 5.06 \times 10^{-7}$ mol/L, $C_{(Ag_2S\,QDs)} = 1.5 \times 10^{-4}$ mol/L, pH = 7.4).

Table 1: Fluorescence quenching constant K_{SV} values of the interaction between Ag_2S QDs and HSA at different temperatures calculated by the Stern-Volmer equation.

T/(K)	Linear equation	K_{SV} ($\times 10^3$ L·mol^{-1})	R^2
313	$y = 1.0 + (5.9 \pm 0.2) \times 10^3 C$	5.9 ± 0.2	0.998
305	$y = 1.0 + (6.7 \pm 0.2) \times 10^3 C$	6.7 ± 0.2	0.996
297	$y = 1.0 + (7.3 \pm 0.3) \times 10^3 C$	7.3 ± 0.3	0.997

quenching only the excited state fluorescent molecule interacts with the quencher [30, 31]. Temperature has a great influence on the quenching process. The decrease of temperature not only reduces the stability of the ground-state compounds, but also reduces the static quenching degree. However, with the increase of temperature, molecular motion will be accelerated due to the decrease of solution viscosity, leading to an increased intermolecular collision rate and fluorescence quenching [32].

The fluorescence quenching data were analyzed by the Stern-Volmer equation:

$$\frac{F_0}{F} = 1 + K_{SV}[Q] = 1 + K_q \tau_0, \quad (1)$$

where F_0 and F are the fluorescence intensities of HSA in the absence and presence of Ag_2S QDs, respectively. K_{SV} is the Stern-Volmer quenching constant, which is a measure parameter of the quenching efficiency [33]. K_q is the biomolecular quenching constant. τ_0 is the lifetime of the fluorescence in the absence of quencher [34], and [Q] is the concentration of Ag_2S QDs. As shown in Figure 4, when the temperature increases, the quenching efficiency decreases obviously, suggesting that static quenching plays a dominant role in this quenching process.

The data of Table 1 indicate that the fluorescence quenching constant K_{SV} of the interaction of Ag_2S QDs with HSA decreased with the increase of temperature (pH = 7.4). According to K_{SV}, when pH = 7.4, K_{SV} is 10^3 orders of magnitude, and the average fluorescence lifetime of biological macromolecules is 10^{-8} s [6], so K_q is larger than the largest diffusion constant. This further confirms that the quenching effect of Ag_2S QDs on HSA is static quenching [34].

3.2.3. The Fluorescence Lifetime. Fluorescence lifetime measurement can provide useful information about the type of molecular interactions, and it is the most effective method to distinguish static and dynamic quenching [10]. Figure 5 shows the fluorescence decay curves of HSA in the absence and presence of Ag_2S QDs. The curves are well fitted with a biexponential function and the average lifetime can be calculated by

$$\tau = \frac{\left(B_1\tau_1^2 + B_2\tau_2^2\right)}{\left(B_1\tau_1 + B_2\tau_2\right)}, \quad (2)$$

where τ_1 represents the shorter lifetime and τ_2 represents the longer one; B_1 and B_2 indicate the amplitudes of fast and slow decay components, respectively.

In order to further verify that the quenching is static but not dynamic, we measured the fluorescence lifetime of HSA in the absence and presence of Ag_2S QDs. The fluorescence lifetime of HSA without Ag_2S QDs was 5.63 ± 0.09 ns, and after the addition of Ag_2S QDs into HSA the fluorescence lifetime was 5.64 ± 0.12 ns. Similar fluorescence lifetime indicated that the quenching effect of Ag_2S QDs on HSA is static.

3.2.4. Thermodynamic Parameters. In order to characterize the binding mode of HSA to Ag_2S QDs, the thermodynamic parameters were analyzed. The standard enthalpy change

Table 2: The thermodynamic parameters of the interaction between Ag_2S QDs and HSA.

T	K_{SV} ($\times 10^3$ L·mol^{-1})	ΔH^θ (KJ·mol^{-1})	ΔS^θ (J·mol^{-1}·K^{-1})	ΔG^θ (KJ·mol^{-1})
313	5.9 ± 0.2	−10.79	−37.80	−22.27
305	6.7 ± 0.2			−22.33
297	7.3 ± 0.3			−22.04

(ΔH^θ) and standard entropy change (ΔS^θ) can be calculated by the thermodynamic equation

$$\ln K^\theta = -\frac{\Delta H^\theta}{RT} + \frac{\Delta S^\theta}{R}. \quad (3)$$

The free energy change (ΔG^θ) was estimated from the following relationship:

$$\Delta G^\theta = \Delta H^\theta - T\Delta S^\theta, \quad (4)$$

where R is the gas constant, 8.314 J mol^{-1} K^{-1}; T is the temperature (K); K^θ is the equilibrium constant at the corresponding temperature, which stands for the static quenching constant (K_{SV}) in the present paper [10]. According to (3) and (4) for plotting the $\ln K^\theta \sim (1/T)$ diagram [33], the value of ΔH^θ was calculated, and then ΔG^θ and ΔS^θ were estimated based on the slope of the curve (Table 2).

From Table 2, it can be seen that when pH = 7.4, ΔH^θ is a negative value (−10.79 KJ·mol^{-1}) and ΔS^θ is a positive value (37.80 J·mol^{-1}·K). With the increase of temperature, ΔG^θ only has a slight change. In these experiments, Ag_2S QDs-HSA complexes underwent both negative enthalpy changes (ΔH^θ) and positive entropy changes (ΔS^θ) (Table 2), demonstrating that the binding interactions are entropically driven. The negative sign for ΔG^θ indicates the spontaneity of the binding of Ag_2S QDs onto HSA. According to the literature [33, 35, 36] and based on the characteristic signs of the thermodynamic parameters during various interactions, the positive enthalpy changes and their values generally represent hydrophobic interaction as the main force. The positive ΔH^θ and negative ΔG^θ indicate that the electrostatic interaction plays major roles in the reaction. Both negative ΔH^θ and ΔG^θ mean that the main force is van der Waals and hydrogen bond interaction. Therefore, from Table 2, it can be seen that the main force between Ag_2S QDs and HSA is electrostatic interaction.

3.2.5. Conformational Changes of HSA Induced by Ag_2S QDs. Raman spectrum is a good tool to study the interaction of protein and nanoparticles [37]. Figure 6 shows the Raman spectrum of HSA in the absence and presence of Ag_2S QDs. The 1655 cm^{-1} band is attributed to amide I, which is characteristic of high α-helical content in HSA. There is no change in the intensity at 1655 cm^{-1} after HSA interaction with Ag_2S QDs, indicating that Ag_2S QDs do not change the

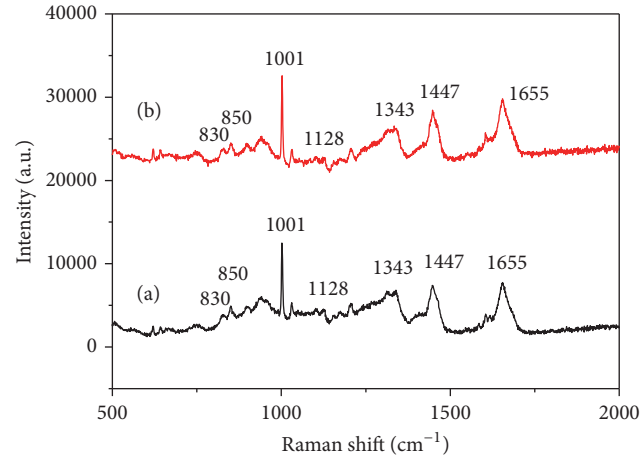

Figure 6: Raman spectra of HSA in the absence (a) and presence (b) of Ag_2S QDs ($C_{(HSA)} = 1.0 \times 10^{-5}$ mol/L, $C_{(Ag_2S)} = 1.0 \times 10^{-4}$ mol/L, pH = 7.4).

α-helical content in HSA. A previous study has revealed that the ratio of the intensity at 850 cm^{-1} to that at 830 cm^{-1} is related to the environment of tyrosine, showing the exposure of hydrophobic groups of HSA [38]. In the present study, the intensity ratio of 850 cm^{-1} to that of 830 cm^{-1} changed from 1.34 to 1.17 after the interaction of HSA with Ag_2S QDs, indicating that the external environment of tyrosine is changed. The 1343 cm^{-1} band assigned to tryptophan or C-H bending is decreased after HSA interaction with Ag_2S QDs. Thus, the presence of Ag_2S QDs can induce alterations in the external environment and structure of HSA.

4. Conclusions

This work has explored the interaction between Ag_2S QDs and HSA, and the results show that the fluorescence quenching effect is enhanced with increasing Ag_2S QDs concentrations, but the enhancement decreases when Ag_2S QDs concentration attained saturation. By using UV-Vis absorption spectra, fluorescence lifetime, Stern-Volmer equation, and thermodynamic equations, we have obtained the Ag_2S QDs and HSA binding fluorescence quenching constant of reaction (K_{SV}), the thermodynamic enthalpy (ΔH^θ), entropy (ΔS^θ), and free energy change (ΔG^θ) values. The results demonstrate the mechanism of static quenching and spontaneous reaction between Ag_2S QDs and HSA as well as their interactions mainly as electrostatic attraction. The Raman spectrum shows that Ag_2S QDs do not change the α-helical content in HSA but alter the external environment of tyrosine and tryptophan or the C-H bending of HSA. The integrated data demonstrate that Ag_2S QDs are a good fluorescence quencher towards proteins such as HSA and they have the potential for the development of ratiometric fluorescent probes.

Competing Interests

The authors declare that there are no competing interests regarding the publication of this paper.

Acknowledgments

This work is financially supported by the National Natural Science Foundation of China (21305049). The authors would like to thank Professor Hanchang Zhu at the College of Foreign Languages, Huazhong Agricultural University, for polishing the English language of the manuscript.

References

[1] N. Xia, B. Zhou, N. Huang, M. Jiang, J. Zhang, and L. Liu, "Visual and fluorescent assays for selective detection of beta-amyloid oligomers based on the inner filter effect of gold nanoparticles on the fluorescence of CdTe quantum dots," *Biosensors and Bioelectronics*, vol. 85, pp. 625–632, 2016.

[2] H. Pei, Y. Zheng, R. Kong, L. Xia, and F. Qu, "Niche nanoparticle-based FRET assay for bleomycin detection via DNA scission," *Biosensors and Bioelectronics*, vol. 85, pp. 76–82, 2016.

[3] Y. Ye, L. Xia, D. Xu, X. Xing, D. Pang, and H. Tang, "DNA-stabilized silver nanoclusters and carbon nanoparticles oxide: a sensitive platform for label-free fluorescence turn-on detection of HIV-DNA sequences," *Biosensors and Bioelectronics*, vol. 85, pp. 837–843, 2016.

[4] Y. Zhou, H. Yin, X. Li, Z. Li, S. Ai, and H. Lin, "Electrochemical biosensor for protein kinase A activity assay based on gold nanoparticles-carbon nanospheres, phos-tag-biotin and β-galactosidase," *Biosensors and Bioelectronics*, vol. 86, pp. 508–515, 2016.

[5] K. Das, S. Sanwlani, K. Rawat, C. R. Haughn, M. F. Doty, and H. B. Bohidar, "Spectroscopic profile of surfactant functionalized CdSe quantum dots and their interaction with globular plasma protein BSA," *Colloids and Surfaces A: Physicochemical and Engineering Aspects*, vol. 506, pp. 495–506, 2016.

[6] X.-C. Shen, X.-Y. Liou, L.-P. Ye, H. Liang, and Z.-Y. Wang, "Spectroscopic studies on the interaction between human hemoglobin and CdS quantum dots," *Journal of Colloid and Interface Science*, vol. 311, no. 2, pp. 400–406, 2007.

[7] Q. Wang, X. Zhang, X. Zhou et al., "Interaction of different thiol-capped CdTe quantum dots with bovine serum albumin," *Journal of Luminescence*, vol. 132, no. 7, pp. 1695–1700, 2012.

[8] Q.-Y. Luo, Y. Lin, J. Peng et al., "Evaluation of nonspecific interactions between quantum dots and proteins," *Physical Chemistry Chemical Physics*, vol. 16, no. 17, pp. 7677–7680, 2014.

[9] H. Wang, L. Shang, P. Maffre et al., "The nature of a hard protein corona forming on quantum dots exposed to human blood serum," *Small*, vol. 12, no. 42, pp. 5836–5844, 2016.

[10] F. Xue, L. Liu, Y. Mi, H. Han, and J. Liang, "Investigation the interaction between protamine sulfate and CdTe quantum dots with spectroscopic techniques," *RSC Advances*, vol. 6, no. 13, pp. 10215–10220, 2016.

[11] Y.-B. Li, H.-X. Zhang, C.-X. Guo et al., "Cytotoxicity and DNA damage effect of TGA-capped CdTe quantum dots," *Chemical Research in Chinese Universities*, vol. 28, no. 2, pp. 276–281, 2012.

[12] W. Xu, T. Du, C. Xu, H. Han, J. Liang, and S. Xiao, "Evaluation of biological toxicity of CdTe quantum dots with different coating reagents according to protein expression of engineering *Escherichia coli*," *Journal of Nanomaterials*, vol. 2015, Article ID 583963, 7 pages, 2015.

[13] J. Wang, R. Liu, and B. Liu, "Cadmium-containing quantum dots: current perspectives on their application as nanomedicine and toxicity concerns," *Mini-Reviews in Medicinal Chemistry*, vol. 16, no. 11, pp. 905–916, 2016.

[14] Y. Tang, J. Hu, X. Yang, and H. Xu, "Biotoxicity of cadmium-based quantum dots and the mechanisms," *Progress in Chemistry*, vol. 26, no. 10, pp. 1731–1740, 2014.

[15] J. Zhang, G. Hao, C. Yao et al., "Albumin-mediated biomineralization of paramagnetic NIR Ag_2S QDs for tiny tumor bimodal targeted imaging *in vivo*," *ACS Applied Materials and Interfaces*, vol. 8, no. 26, pp. 16612–16621, 2016.

[16] J. Song, C. Ma, W. Zhang et al., "Bandgap and structure engineering via cation exchange: from binary Ag_2S to ternary $AgInS_2$, quaternary AgZnInS alloy and AgZnInS/ZnS core/shell fluorescent nanocrystals for bioimaging," *ACS Applied Materials & Interfaces*, vol. 8, no. 37, pp. 24826–24836, 2016.

[17] C. Li, Y. Zhang, M. Wang et al., "In vivo real-time visualization of tissue blood flow and angiogenesis using Ag_2S quantum dots in the NIR-II window," *Biomaterials*, vol. 35, no. 1, pp. 393–400, 2014.

[18] J. Gao, C. Wu, D. Deng, P. Wu, and C. Cai, "Direct synthesis of water-soluble aptamer-Ag_2S quantum dots at ambient temperature for specific imaging and photothermal therapy of cancer," *Advanced Healthcare Materials*, vol. 5, no. 18, pp. 2437–2449, 2016.

[19] J. Zhang, C. Hu, and B. Zhang, "Facile synthesis of paramagnetic silver sulfide quantum dots for tumor targeted bimodal imaging," *Nanomedicine: Nanotechnology, Biology and Medicine*, vol. 12, no. 2, p. 505, 2016.

[20] W. Ouyang and J. Sun, "Biosynthesis of silver sulfide quantum dots in wheat endosperm cells," *Materials Letters*, vol. 164, pp. 397–400, 2016.

[21] Q. Xiao, S. Huang, W. Su et al., "Systematically investigations of conformation and thermodynamics of HSA adsorbed to different sizes of CdTe quantum dots," *Colloids and Surfaces B: Biointerfaces*, vol. 102, pp. 76–82, 2013.

[22] J. Nilvebrant, T. Alm, S. Hober, and J. Löfblom, "Engineering bispecificity into a single Albumin-Binding domain," *PLOS ONE*, vol. 6, no. 10, Article ID e25791, 2011.

[23] F. Kratz, "Albumin as a drug carrier: design of prodrugs, drug conjugates and nanoparticles," *Journal of Controlled Release*, vol. 132, no. 3, pp. 171–183, 2008.

[24] U. Kragh-Hansen, V. T. G. Chuang, and M. Otagiri, "Practical aspects of the ligand-binding and enzymatic properties of human serum albumin," *Biological and Pharmaceutical Bulletin*, vol. 25, no. 6, pp. 695–704, 2002.

[25] W. Li, D. Chen, H. Wang et al., "Quantitation of albumin in serum using 'turn-on' fluorescent probe with aggregation-enhanced emission characteristics," *ACS Applied Materials and Interfaces*, vol. 7, no. 47, pp. 26094–26100, 2015.

[26] N. Giamblanco, N. Tuccitto, G. Zappalà, G. Sfuncia, A. Licciardello, and G. Marletta, "Chelating surfaces for native state proteins patterning: the human serum albumin case," *ACS Applied Materials and Interfaces*, vol. 7, no. 41, pp. 23353–23363, 2015.

[27] H. Chen, B. Li, M. Zhang et al., "Characterization of tumor-targeting Ag_2S quantum dots for cancer imaging and therapy in vivo," *Nanoscale*, vol. 6, no. 21, pp. 12580–12590, 2014.

[28] Y. V. Il'ichev, J. L. Perry, and J. D. Simon, "Interaction of ochratoxin a with human serum albumin. Preferential binding of the dianion and pH effects," *Journal of Physical Chemistry B*, vol. 106, no. 2, pp. 452–459, 2002.

[29] C. Wang, Y. Wang, L. Xu et al., "Facile aqueous-phase synthesis of biocompatible and fluorescent Ag_2S nanoclusters for bioimaging: tunable photoluminescence from red to near infrared," *Small*, vol. 8, no. 20, pp. 3137–3142, 2012.

[30] H. Yan, J. Wu, G. Dai et al., "Interaction mechanisms of ionic liquids [C nmim]Br (n=4, 6, 8, 10) with bovine serum albumin," *Journal of Luminescence*, vol. 132, no. 3, pp. 622–628, 2012.

[31] R. Freeman, T. Finder, L. Bahshi, R. Gill, and I. Willner, "Functionalized CdSe/ZnS QDs for the detection of nitroaromatic or RDX explosives," *Advanced Materials*, vol. 24, no. 48, pp. 6416–6421, 2012.

[32] G. Katsukis, J. Malig, C. Schulz-Drost, S. Leubner, N. Jux, and D. M. Guldi, "Toward combining graphene and QDs: assembling CdTe QDs to exfoliated graphite and nanographene in water," *ACS Nano*, vol. 6, no. 3, pp. 1915–1924, 2012.

[33] J. Tian, J. Liu, W. He, Z. Hu, X. Yao, and X. Chen, "Probing the binding of scutellarin to human serum albumin by circular dichroism, fluorescence spectroscopy, FTIR, and molecular modeling method," *Biomacromolecules*, vol. 5, no. 5, pp. 1956–1961, 2004.

[34] Z.-Q. Xu, L. Lai, D.-W. Li et al., "Toxicity of CdTe QDs with different sizes targeted to HSA investigated by two electrochemical methods," *Molecular Biology Reports*, vol. 40, no. 2, pp. 1009–1019, 2013.

[35] C. Zheng, H. Wang, W. Xu, C. Xu, J. Liang, and H. Han, "Study on the interaction between histidine-capped Au nanoclusters and bovine serum albumin with spectroscopic techniques," *Spectrochimica Acta—Part A: Molecular and Biomolecular Spectroscopy*, vol. 118, pp. 897–902, 2014.

[36] P. D. Ross and S. Subramanian, "Thermodynamics of protein association reactions: forces contributing to stability," *Biochemistry*, vol. 20, no. 11, pp. 3096–3102, 1981.

[37] L. Liu, L. Chen, J. Liang, L. Liu, and H. Han, "A novel ratiometric probe based on nitrogen-doped carbon dots and rhodamine b isothiocyanate for detection of Fe^{3+} in aqueous solution," *Journal of Analytical Methods in Chemistry*, vol. 2016, Article ID 4939582, 7 pages, 2016.

[38] N.-T. Yu and B. H. Jo, "Comparison of protein structure in crystals and in solution by laser Raman scattering: I. Lysozyme," *Archives of Biochemistry and Biophysics*, vol. 156, no. 2, pp. 469–474, 1973.